35th Annual International Conference of the IEEE EMBS
Osaka, Japan, 3 - 7 July, 2013

On High-Resolution Image Estimation using Low-Resolution Brain MRI

François Rousseau[1], Daniel Gounot[1] and Colin Studholme[2]

Abstract— **In the context of medical imaging, super-resolution (SR) is currently a promising post-processing technique to increase the image resolution. However, although many SR methods have been proposed in the literature, the gain of this type of approach in a real situation has not been precisely quantified. In this work, we evaluate image acquisition protocols and SR algorithms using in-vivo brain MR data as gold standard. The results show that using orthogonal image acquisition protocols lead to better reconstructed images than overlapping parallel low-resolution image stacks. Moreover, if the preprocessing steps (such as image denoising and intensity correction) are carefully performed, there is no significant differences between the evaluated SR algorithms.**

I. INTRODUCTION

3D MR acquisitions such as MPRAGE or SPGR provide an efficient route to providing high isotropic resolution with optimal collection of signal over a few minutes. However, this is a still significant acquisition time in the context of clinical imaging where motion during any of the 3D acquisition period will impact the entire volumetric scan. As a result, multi-slice imaging is still a preferred route in many clinical settings since slice imaging time is much less than a full volume, and motion, when it occurs, only impacts a subset of slices. However, in order to ensure acceptable signal to noise in multi-slice acquisitions slice thicknesses are often many times the in-plane pixel size leading to highly anisotropic resolution.

To overcome this relative poor resolution, image processing algorithms such as super resolution (SR) techniques have been explored during the last decade. The core principle of SR methods is to combine several low-resolution images of the same scene taken at different view points to create a high resolution image. Such techniques are of primary interest in medical imaging where image resolution remains a key point for many image analysis steps such as segmentation.

In MRI, several image acquisition protocols can be considered appropriate for SR processing. It is important to notice that in MRI, the best that can be aimed for in the terms of resolution enhancement to within plane resolution is image deblurring due to the band limited nature of the acquired signal used to form each slice. However, in cases of suitable slice profile, SR techniques can be used to increase the resolution in the inter-slice direction. For instance, in [5], Greenspan *et al.* have proposed an interleave strategy which consists in combining overlapping parallel low-resolution image stacks to reconstruct a high-resolution image. In contrast during fetal brain MRI studies [15], usual image acquisition protocols consist in acquiring at least three orthogonal anatomical images in each direction (axial, coronal and sagittal) to provide the radiologist with an overview of the fetal brain. In this context resolution is not simply provided by repeated but shifted acquisitions, but from ani-isotropic acquisitions with complementary orientations that can be combined to provide isotropic resolution. SR algorithms have been evaluated in [11] to study the influence of the number of input images and image noise level on the quality of reconstructed images.

After having determined the image acquisition protocol, another key step in SR algorithms is the mathematical methodology used to recover the high resolution image using a dedicated observation model. As an example, the reconstruction algorithm used in [5] was based on the iterative back-projection. Other reconstruction methods such as algebraic methods or regularized techniques have also been explored in MRI context [9]. A review of SR techniques in medical imaging can be found in [6]. Moreover, other image modeling strategies have been recently investigated to increase brain MR image resolution by using inter-modality priors [10], groupwise analysis [11] or dictionary-based approach [14].

Another key question about SR in MRI is the potential gain in resolution that can be achieved. In the general context of SR, Baker and Kanade in [1] have shown that ”the reconstruction constraints provide less and less useful information as the magnification factor increases”. Typically, the maximum magnification factor is smaller than 2. This has led them to propose a supervised reconstruction technique to introduce details in the reconstructed images. The study of gain resolution in the context of MRI has been done by few researchers [8], [16], [9]. However, despite all the reconstruction methods proposed in the literature, it is not clear what can be the gain in resolution in a practical context, or what is the optimal image acquisition protocol.

Lastly, SR techniques are usually quantitatively evaluated using synthetic images or phantoms and visually evaluated on real datasets. Using synthetic data provides only information on ”possible” performance of SR algorithms. Indeed, such evaluation is an ”inverse crime” since the same observation model is used for low resolution image synthesis and SR reconstruction (*i.e.* to invert data in an inverse problem).

The research leading to these results has received funding from the European Research Council under the European Communitys Seventh Framework Programme (FP7/20072013 Grant Agreement No. 207667). This work is also funded by NIH Grants NIH/NINDS R01 NS 061957 and NIH/NINDS R01 NS 055064.

[1]F. Rousseau and D. Gounot are with the ICube laboratory, Université de Strasbourg, CNRS, UMR 7357, Strasbourg, France. rousseau at unistra.fr

[2]C. Studhome is with the Depts. of Pediatrics and Bioengineering, University of Washington, Seattle, USA.

978-1-4577-0216-7/13/$26.00 ©2013 IEEE

Using real MR images of phantoms is also not a fully satisfactory solution for SR evaluation because such phantoms exhibit image properties (such as large uniform areas and strong edges) that rarely happen in in-vivo MR images. As a consequence, there is a clear need for the community to develop gold standard images based on in-vivo MR data for SR algorithm benchmarking.

The purpose of this experimental work is to provide new insights on effective gain resolution when considering in-vivo brain MR data. This article presents a comparison of several SR techniques and image acquisition protocols evaluated on in-vivo brain MRI. Section II describes the image processing problem of SR, highlighting the definition of data discrepancy functionals and regularization functionals. Section III presents MR data and the pre-processing steps (such as denoising, intensity correction and registration) required for the construction of a gold standard and for application of SR techniques to MR images. Lastly, Section IV describes comparison results of image acquisition protocols and SR algorithms using in-vivo gold standard brain MR image.

II. Super-resolution

SR is usually expressed as a problem of estimating a quantity degraded by a linear operator and corrupted by noise :

$$\mathbf{y} = H\mathbf{x} + n \tag{1}$$

where H is a linear operator linking the unknown quantity $\mathbf{x} \in \mathcal{X}$ to the observed data $\mathbf{y} \in \mathcal{Y}$ and n is the noise. This mathematical formulation is commonly encountered in many other image processing problems such as denoising, deconvolution, segmentation, inpainting.

Using the observation model described by Equation (1), a straightforward definition of the data discrepancy functional is:

$$D(\mathbf{x}, \mathbf{y}) = \psi(H\mathbf{x} - \mathbf{y}). \tag{2}$$

ψ is usually set as a quadratic functional by assuming that the image noise n follows a Gaussian distribution. Another common choice for ψ is the $\mathbf{L}^1$ norm as it is usually more robust to outliers. In this work, we have compared these two data discrepancy functionals ($\mathbf{L}^2$ and $\mathbf{L}^1$ norms).

However, an estimate of $\mathbf{x}$ (denoted as $\hat{\mathbf{x}}$) cannot be uniquely determined by minimizing $D(\mathbf{x}, \mathbf{y})$ since it is an ill-posed problem. For such inverse problems, some form of regularization plays a crucial role and must be included in the cost function to stabilize the problem or constrain the space of solutions. One popular variational regularization functional relies on the total variation:

$$J_{TV}(\mathbf{x}) = \int |\nabla \mathbf{x}(\mathbf{v})| d\mathbf{v} \tag{3}$$

where $\mathbf{v}$ is a voxel of the image. Charbonnier *et al.* in [2] have proposed several edge-preserving regularization functionals from which we select one to use in our experiments:

$$J_{Ch}(\mathbf{x}) = \int \phi(\nabla \mathbf{x}(\mathbf{v})) d\mathbf{v} \tag{4}$$

with $\phi(t) = 2\sqrt{1+t^2} - 2$. In this work, we have considered these two regularization functionals (J_{TV} and J_{Ch}).

The overall energy ($D(\mathbf{x}, \mathbf{y}) + \lambda J(\mathbf{x})$) is minimized using a gradient descent algorithm. The parameter λ acting as a trade-off between the data-fidelity term and the regularization has been chosen empirically by maximizing the peak signal to noise ratio (PSNR) between the gold standard and the reconstructed image.

III. Experimental setting

A. Data

In this work, experiments have been carried out on a set of T1-weighted MPRAGE images of the same acquired in one session on a 3T Siemens Verio MRI Scanner (SIEMENS, Erlangen, Germany). The following pulse sequence parameters were used: repetition time = 2800 ms, echo time = 2.67 ms, inversion time = 1140 ms, field of view = 256×256 mm^2. Isotropic images (voxel resolution : $1 \times 1 \times 1$ mm^3) were acquired to provide a gold standard image (also called ground truth in the literature) for evaluation purpose. Overlapping anisotropic images (voxel resolution : $1 \times 1 \times 2$ mm^2) in the three directions (axial, sagittal and coronal) were used as low resolution image inputs to SR algorithms.

B. Preprocessing

A key point in evaluating SR algorithms is to make sure that the gold standard and the reconstructed images are similar. In order to do so, motion and intensity corrections are required. The following (freely available) image processing pipeline have been applied to the set of MR images: 1) brain extraction using a supervised patch-based technique [12], 2) bias correction using N4ITK [17], 3) a groupwise midway histogram equalization similar to the algorithm proposed in [4], 4) image denoising using nonlocal means [3] , 5) and motion estimation (rigid transforms) using Rview[1]. Steps 1,3,4 make use of algorithms implemented in the Baby Brain Toolkit (BTK) [13].

The first step consists in extracting the brain from the MR images. In this study, this is done by applying a supervised patch-based label propagation technique. Briefly, this algorithm makes use of local similarities between the image to be segmented and the images contained in a MRI-derived anatomy textbook. Using such patch-based local similarities has shown to be very effective for brain segmentation [12].

The second step of the pipeline is the correction of intensity bias due to radio-frequency field inhomogeneities. In this work, we have used the N4ITK algorithm proposed in [17] which is basically an implementation of the well-known N3 algorithm using ITK. The purpose of this algorithm is to correct smooth variation of the intensity over the tissue that should have intensity close to uniform.

The third step consists in making the intensity of brain tissues consistent for each image of the data set. This is performed in a groupwise fashion using midway histogram equalization [4]. Consider two images I_1 and I_2, whose

[1] http://rview.colin-studholme.net

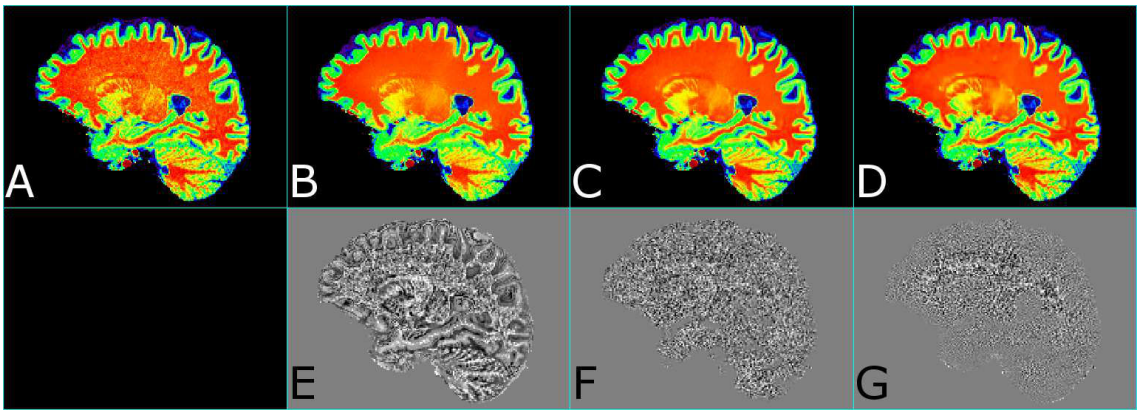

Fig. 1. Comparison of denoising algorithms for gold standard building on sagittal view. Images are displayed using the same contrast scale. First row: A) original image, denoised images using B) SUSAN-FSL, C) BTK-NLM [13], D) PRINLM [7]. Second row: difference images (E,F,G) between the original image (A) and the denoised images (B,C,D). Following the "noise method" evaluation approach, the BTK version of the nonlocal means algorithm (C,F) provides the most satisfactory results.

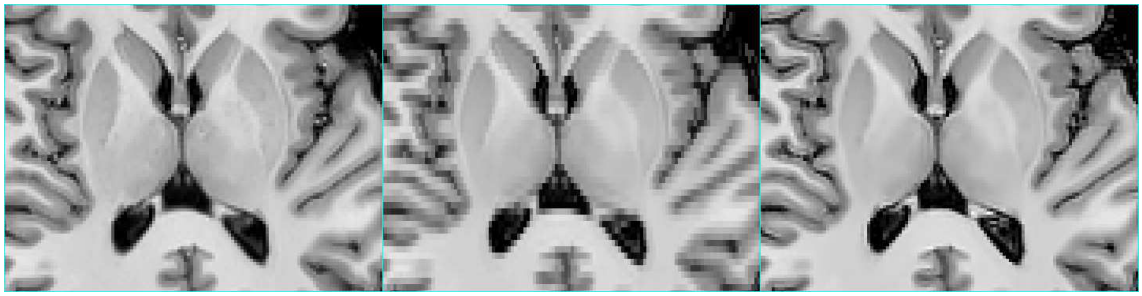

Fig. 2. Close up of images. Left: gold standard (isotropic denoised image), middle: low-resolution coronal image, right: SR image.

cumulative histograms are M_1 and M_2. In order to make them have the same histogram, a cumulative histogram M has to be chosen so that the two images have a new cumulative histogram equal to M by applying a contrast change. The intermediate cumulative histogram M can be constructed as follows:

$$M = \left(\frac{M_1^{-1} + M_2^{-1}}{2} \right)^{-1}. \quad (5)$$

Then, each image I_i is replaced by $\phi_i(I_i)$ where $\phi_i = M^{-1} \circ M_i$. It is straightforward to extend this histogram equalization technique to a set of N images by considering an intermediate cumulative histogram defined as follows:

$$M = \left(\frac{\sum_{i=1}^{N} M_i^{-1}}{N} \right)^{-1}. \quad (6)$$

In order to form an optimal gold standard image, the fourth step of the pipeline is a denoising step. A nonlocal means technique has been applied and the result has been carefully checked in order to avoid any loss of details in the high resolution image. We have compared three denoising algorithms (SUSAN-FSL[2]), BTK version of the nonlocal means (BTK-NLM) [13], prefiltered rotationally invariant nonlocal means filter (PRINLM) [7] using the "noise method", *i.e.* by analyzing visually the difference images between the original image and the denoised images. Results are shown on Figure 1. The best denoised image is the one where the difference image is as similar to a pure noise image as possible, *i.e.* intensities of the difference image should not depend on the brain tissues. While the SUSAN-FSL algorithm provides less optimal results, the denoised images using PRINLM and BTK-NLM are good candidates for SR gold standard building. Moreover, it has to be noticed that denoising low resolution images helps the SR algorithms to converge to a better estimate of the high resolution image. As a consequence, all the images used in this study have been denoised using the nonlocal means technique (BTK-NLM).

The last step of the proposed pipeline is the motion estimation. This is a key point in SR techniques since a poor estimation of motion leads to an incorrect matrix H. Therefore, SR algorithms are highly dependent on this step. In this work, rigid transforms have been estimated between the gold standard image and the low resolution images by maximizing the Normalized Mutual Information as implemented in the standard registration within Rview.

IV. Results

For quantitative comparison, the PSNR is reported in decibels (dB):

$$PSNR = 10 \log_{10} \left(\frac{d^2}{|\Omega|^{-1} \sum_{\mathbf{v} \in \Omega} (\mathbf{x}(\mathbf{v}) - \hat{\mathbf{x}}(\mathbf{v}))^2} \right) \quad (7)$$

[2]http://fsl.fmrib.ox.ac.uk

where d is the reference image dynamic. The PSNR is related to the mean square error between the gold standard and the reconstructed image. Because the brain is the object of interest in this study, the PSNR has to be computed only on brain tissues.

The brain mask estimated using the patch-based labeling algorithm cannot be used for SR evaluation purpose. Indeed, some tissues or structures such blood vessels (due to blood flow) and fat (due to chemical shift) have different intensity appearances depending on the orientation of the image acquisition (axial, coronal or sagittal). Then, in order to perform a fair comparison between image acquisition protocols, it was necessary to build a mask in which brain tissues share the same appearance whatever the direction used for image acquisition.

To do so, all low resolution images have been registered to the gold standard image. Then, considering all the images (*i.e.* the gold standard and the registered images), an image of the intensity variance is computed at each voxel. High variance means that images may not share the same intensity appearance at a particular location. Then, the brain mask used for evaluation is the intersection (*i.e.* logical operator AND) of the brain mask obtained using the supervised patch-based labeling technique [12] and a thresholded version of the variance map.

TABLE I

PSNR RESULTS DEPENDING ON THE DATA DISCREPANCY FUNCTIONAL ψ, THE REGULARIZATION TERM J AND THE ACQUISITION PROTOCOL.

ψ	J	axial	coronal	sagittal	ortho3	ortho6
$\mathbf{L}^2$	J_{TV}	35.02	35.00	33.93	37.15	37.15
$\mathbf{L}^1$	J_{TV}	34.94	34.58	33.12	36.98	37.49
$\mathbf{L}^2$	J_{Ch}	35.48	34.78	34.07	37.47	37.49
$\mathbf{L}^1$	J_{Ch}	34.82	34.59	33.14	36.91	37.52

The analysis of PSNR results (see Table I) shows that using orthogonal acquisitions leads to better reconstruction results than using overlapping anisotropic images in the same direction (axial, coronal or sagittal). This was expected because images were acquired using 3D MPRAGE sequences. This means that only orthogonal acquisitions provide complementary information in the k-space. Acquiring shifted acquisitions helps the increase of the signal to noise ratio and in this case, the SR methods acts as deblurring technique. Moreover, the performance of the SR algorithms are very similar using 3 or 6 orthogonal images with the proposed preprocessing pipeline. Figure 2 shows an example of SR reconstruction compared to the gold standard (left column) and low-resolution anisotropic coronal image.

V. CONCLUSIONS

The purpose of this work has involved the study of protocols for image acquisition and SR reconstruction algorithms using in vivo brain MRI. We have proposed a image processing pipeline carefully designed to take into account possible distortions such as intensity variations of brain tissues. The results highlighted some significant differences in the quality of reconstructions based on different acquisition protocols. Future work will involve the construction of a larger set of images (for example by using a wider range of image resolutions) to provide the community with a consistent means for evaluating SR algorithms applied to different forms multi-slice MRI data seen in clinical practice.

REFERENCES

[1] S. Baker, T. Kanade. "Limits on Super-Resolution and How to Break Them," IEEE Trans. on Pattern Analysis and Machine Intelligence, vol. 24, no. 9, pp: 1167-1183, 2002.

[2] P. Charbonnier, L. Blanc-Feraud, G. Aubert & M. Barlaud. "Deterministic edge-preserving regularization in computed imaging," IEEE Transactions on Image Processing, vol. 6, no. 2, pp. 298-311, 1997.

[3] P. Coupé, P. Yger, S. Prima, P. Hellier, C. Kervrann, C. Barillot. "An Optimized Blockwise Non Local Means Denoising Filter for 3D Magnetic Resonance Images," IEEE Trans. on Medical Imaging, vol. 27, no. 4, pp. 425-441, 2008.

[4] J. Delon. "Midway Image Equalization," Journal of Mathematical Imaging and Vision, vol. 21, pp. 119-134, 2004.

[5] H. Greenspan, G. Oz, N. Kiryati, S. Peled. "MRI inter-slice reconstruction using super-resolution, " Magnetic Resonance Imaging, vol. 20, pp. 437-446, 2002.

[6] H. Greenspan. "Super-Resolution in Medical Imaging," The Computer Journal, vol. 52, no.1, pp. 43-63, 2009.

[7] J. V. Manjon, P. Coupé, A. Buades, D. L. Collins, M. Robles. "New Methods for MRI Denoising based on Sparseness and Self-Similarity," Medical Image Analysis, vol. 16, no. 1, pp. 18-27, 2012.

[8] G.S. Mayer, E.R. Vrscay. "Measuring information gain for frequency-encoded super-resolution MRI," Magnetic Resonance Imaging, vol. 25, pp. 1058-1069, 2007.

[9] E. Plenge, D.H.J. Poot, M. Bernsen, G. Kotek, G. Houston, P. Wielopolski, L. van der Weerd, W.J. Niessen, E. Meijering. "Super-Resolution Methods in MRI: Can They Improve the Trade-Off Between Resolution, Signal-to-Noise Ratio, and Acquisition Time?," Magnetic Resonance in Medicine, vol. 68, no. 6, pp. 19831993, 2012.

[10] F. Rousseau. "A non-local approach for image super-resolution using intermodality priors," Medical Image Analysis, vol. 14, no. 4, pp. 594-605, 2010.

[11] F. Rousseau, K. Kim, C. Studholme, M. Koob, J.-L. Dietemann. "On Super-Resolution for Fetal Brain MRI," Medical Image Computing and Computer Assisted Intervention, Springer-Verlag, Lecture Notes in Computer Science, vol. 6362, pp. 355-362, 2010.

[12] F. Rousseau, P. Habas, C. Studholme. "A supervised patch-based approach for human brain labeling," IEEE Transactions on Medical Imaging, vol. 30, no. 10, pp. 1852–1862, 2011.

[13] F. Rousseau, E. Oubel, J. Pontabry, M. Schweitzer, C. Studholme, M. Koob, J.-L. Dietemann. "BTK: An Open-Source Toolkit for Fetal Brain MR Image Processing," Computer Methods and Programs in Biomedicine, vol. 109, no. 1, pp. 65-73, 2013.

[14] A. Rueda, N. Malpica, E. Romero. "Single-image super-resolution of brain MR images using overcomplete dictionaries," Medical Image Analysis, vol. 17, no. 1, pp. 113-132, 2013.

[15] C. Studholme. "Mapping Fetal Brain Development In Utero Using Magnetic Resonance Imaging: The Big Bang of Brain Mapping," Annual Review of Biomedical Engineering, vol. 13, pp. 345-368, 2011.

[16] Q.M. Tieng, G.J. Cowin, D.C. Reutens, G.J. Galloway, V. Vegh. "MRI Resolution Enhancement: How Useful are Shifted Images Obtained by Changing the Demodulation Frequency?," Magnetic Resonance in Medicine, vol. 65, pp. 664-672, 2011.

[17] N.J. Tustison, B.B. Avants, P.A. Cook, Y. Zheng, A. Egan, P.A. Yushkevich, J.C. Gee. "N4ITK: improved N3 bias correction," IEEE Trans on Medical Imaging, vol. 29, no. 6, pp. 1310-1320, 2010.